

RESEARCH ARTICLE

Open Access



Ecological adaptations of amphibians to environmental changes along an altitudinal gradient (Case Study: *Bufo gargarizans*) from phenotypic and genetic perspectives

Yonggang Niu^{1*} , Xuejing Zhang², Haiying Zhang¹, Shengkang Men², Tisen Xu¹, Li Ding³, Xiangyong Li¹, Lei Wang¹, Huisong Wang¹, Kenneth B. Storey⁴ and Qiang Chen²

Abstract

Background Organisms have evolved a range of phenotypic and genetic adaptations to live in different environments along an altitudinal gradient. Herein, we studied the widely distributed Chinese toad, *Bufo gargarizans*, as a model and used an integrated phenotype-genotype approach to assess adaptations to different altitudinal environments.

Results Comparison of populations from four altitudes (50 m, 1200 m, 2300 m, and 3400 m) showed more effective defenses among high-altitude toads. These included thickened epidermis, more epidermal capillaries and granular glands, greater gland size in skin, and higher antioxidant enzyme activities in plasma. High-altitude toads also showed increased erythrocytes and hematocrit and elevated hemoglobin concentration, potentially improving oxygen delivery. Elevated altitude led to a metabolic shift from aerobic to anaerobic metabolism, and high-altitude populations favored carbohydrates over fatty acids to fuel for energy metabolism. Differentially expressed genes were associated with adaptive phenotypic changes. For instance, expression of genes associated with fatty acid metabolism showed greater suppression at high altitude (3400 m), consistent with decreased flux of β -hydroxybutyric acid and lower free fatty acids levels. Moreover, down-regulation of genes involved in carbon metabolism processes at high altitude (3400 m) were coincident with reduced TCA cycle flux. These results suggest that high-altitude toads adopt a metabolic suppression strategy for survival under harsh environmental conditions. Moreover, the hypoxia-inducible factor signaling cascade was activated at high altitude.

Conclusions Collectively, these results advance our comprehension of adaptation to high-altitude environments by revealing physiological and genetic mechanisms at work in Chinese toads living along altitudinal gradients.

Keywords *Bufo gargarizans*, Altitudinal gradient, Phenotypic traits, Transcriptome, Adaptation

*Correspondence:

Yonggang Niu
yonggangniu@126.com

Full list of author information is available at the end of the article



© The Author(s) 2024. **Open Access** This article is licensed under a Creative Commons Attribution-NonCommercial-NoDerivatives 4.0 International License, which permits any non-commercial use, sharing, distribution and reproduction in any medium or format, as long as you give appropriate credit to the original author(s) and the source, provide a link to the Creative Commons licence, and indicate if you modified the licensed material. You do not have permission under this licence to share adapted material derived from this article or parts of it. The images or other third party material in this article are included in the article's Creative Commons licence, unless indicated otherwise in a credit line to the material. If material is not included in the article's Creative Commons licence and your intended use is not permitted by statutory regulation or exceeds the permitted use, you will need to obtain permission directly from the copyright holder. To view a copy of this licence, visit <http://creativecommons.org/licenses/by-nc-nd/4.0/>.

Background

Environmental conditions change with altitude and the elevation gradient provides one of the most potent “natural experiments” for testing ecological and evolutionary adaptation of animals to geophysical influences [1]. Multiple selection pressures at high altitude include hypoxia, low temperatures, and increased ultraviolet radiation (UVR), and all can affect the survival, reproduction, and distribution of animals. Although the severity of environmental challenges increases with altitude, animals are able to survive and thrive for generations due to adaptive mechanisms occurring at morphological, physiological, biochemical, and molecular levels [2].

Amphibian skin is directly exposed to the environment and forms the first protective barrier against pathogens [3] while also providing additional functions including water uptake, respiration, antimicrobial actions and innate immune protection [4]. Changes in the external environment are known to have an impact on skin morphology, such as changing the thickness of skin layers [5], the number and morphology of glands [6, 7], and the content of melanin [8]. Pigments in the epidermis or/and dermis help amphibians to adapt to different conditions, and these can disperse throughout the cytoplasm, darkening the skin, and thereby improving thermoregulation as temperature decreases [9]. For instance, the Xizang plateau frogs, *Nanorana parkeri*, living at high altitude have more epidermal capillaries, granular glands (GGs), and skin pigments than frog species living at lower altitude [10] and this provides morphological evidence of adaptation to the cold and UVR stresses occurring at high altitude. However, in the previous study, the skin morphology of different frog species, rather than conspecifics living at different altitudes, was compared so this does not rule out interference from the species' own genetic background. Overall, exploring skin phenotypes within a species along an altitudinal gradient can provide insights into how organisms adapt to extreme environments at high altitudes.

Several studies have shown that changes in hematological characteristics, such as hemoglobin concentration ([Hb]), hematocrit (Hct), and red blood cell (RBC) count, can improve the oxygen-carrying capacity of blood and contribute to successful life for ectothermic vertebrates living at high altitudes [11–13]. For example, compared to individuals living at low altitude, high-altitude frogs, *Pelophylax nigromaculatus*, showed a significant increase in Hct and [Hb] [14]. As anticipated, we previously found that values of [Hb], Hct, and RBCs in high-altitude frogs, *N. parkeri*, were significantly higher than those in low-altitude individuals [15]. Although high-altitude toads, *Bufo gargarizans*, also show higher [Hb], Hct, and RBCs than low-altitude conspecifics [16], little is known about

the changes in hematological parameters in response to altitudinal gradients.

Apart from unique adaptations in oxygen transport properties, tolerance of hypoxia and low temperature at high altitudes also requires metabolic remodeling at the cell and organ level in order to maintain functional integrity. This can be accomplished by three core adaptations: metabolic rate depression, tolerance of accumulated metabolic by-products, and enhanced defenses against cellular damage (e.g. avoidance and/or repair) [17]. For instance, highland-dwelling lizards, *Phrynocephalus erythrurus*, showed markedly reduced mitochondrial respiration rates but increased lipid mobilization versus their low-altitude relatives [18]. Moreover, in a recent study, we found that high-altitude lizards, *Phrynocephalus vlangalii*, preferred carbohydrates over lipids as their primary fuel, as manifested by lower levels of free fatty acids (FFA) and β -hydroxybutyric acid (β -HB) but no significant changes in most intermediary metabolites of glycolysis and the tricarboxylic acid (TCA) cycle [19]. However, the effects of an altitudinal gradient on metabolite concentrations are not yet well understood in amphibians and no information appears to be available on altitude-related changes in the network of the central metabolic pathway (CMP). Despite a proposal that high-altitude environments can disrupt redox homeostasis in the body, organisms are fortunate to be equipped with well-developed antioxidant defense systems to detoxify free radicals and defend cell molecules, membranes, and organelles from damage [20]. For instance, the high-altitude indigenous frogs, *N. parkeri*, adapt to extreme environments by up-regulating the activity of antioxidant enzymes [15]. Nevertheless, studies exploring oxidative stress and antioxidant defenses in amphibians along an altitudinal gradient are still rare. Addressing the relationship among altitudinal gradients and these physiological and biochemical indices can increase our current knowledge about evolutionary adaptations in ectothermic vertebrates.

In recent years, rapid advances in “omics” technologies, such as genomics, transcriptomics, proteomics, and metabolomics [21], have been a boon to our fundamental understanding of the molecular mechanisms supporting high-altitude adaptation. For instance, transcriptome analysis revealed that high altitude-dwelling lizards *P. erythrurus* and frogs *Rana kukunoris* have an accelerated evolutionary rate as compared with their respective lowland-dwelling counterparts and identified three major gene functions: response to hypoxia, energy metabolism, and response to UVR damage that are likely contributors to high-altitude adaptation [22]. A comparative transcriptome analysis showed that expression of genes related to nutrient metabolism differed significantly

between high- and low-altitude populations of the toad, *B. gargarizans* [23]. Furthermore, multi-tissue transcriptome profiling indicated that genes associated with muscle contraction and nutrient metabolism were down-regulated in the heart and liver of high-altitude toads as compared to low-altitude individuals [24]. However, our understanding of adaptations to different altitudinal environments by ectothermic vertebrates remains limited, especially for amphibians distributed along an altitudinal gradient. Moreover, studies that reveal mechanisms of adaptation to diverse environment conditions by combining phenotypic traits and genetic evidence are scarce.

One species that is particularly suited for exploring the eco-physiological adaptations needed by amphibians to thrive in diverse environments is the Chinese toad, *B. gargarizans* (Bufonidae, Bufo), that has a wide distribution ranging from latitude 20°N to 50°N and its whole genome has been sequenced [25]. The phylogeny of *B. gargarizans* was well resolved [26], and *B. gargarizans* is now classified as a single species and is no longer divided into subspecies [27]. Population structure and genetic diversity analysis also showed that Chinese toads are divided into three main clusters in China: western, central-eastern, and northeastern, and that their migratory routes include from west to central-east and from central-east to northeast [28]. Moreover, comparative studies at three altitudes (790 m, 1500 m, and 2500 m) showed that the expression of genes related to metabolism and response to UVR were altered along the altitudinal gradient, which plays a crucial role in high-altitude adaptation of this species [29]. Although toads living at lower altitude grow faster and exercise less, those individuals living at different altitudes display similar maintenance metabolic rates, which did not support the metabolic cold adaptation hypothesis [30]. At higher altitudes, these toads are subject to various environmental stresses, but there is a limited understanding of the phenotypic characterization and genetic mechanisms responsible for their adaptations to natural environments along an altitudinal gradient.

In the present study, we hypothesized that Chinese toads have developed a suite of phenotypic traits to adapt to their environments along an altitudinal gradient, including (1) enhanced defenses and non-aggravated damage by thickening the epidermis, enriching cutaneous glands and improving antioxidant defenses; (2) increased heat absorption depending on increased melanin and/or darker skin tone; (3) facilitated gas exchange and improved oxygen delivery through richer cutaneous capillaries, increased RBCs counts, higher [Hb] and lower Hct; and (4) metabolic remodeling manifested by a shift from aerobic to anaerobic metabolism and a greater reliance on carbohydrates as a fuel source. From

a perspective of gene expression regulation, hypoxia-associated signaling cascades and the immune system were largely activated, whereas genes involved in energy metabolism processes may be down-regulated to reduce metabolic costs. To test our hypothesis, we collected adult male Chinese toads *B. gargarizans* from four altitudes (50 m, 1200 m, 2300 m, 3400 m above sea level (a.s.l.)) (Fig. 1) and compared skin histology, hematological parameters, antioxidant defense systems, oxidative damage, and metabolite levels in the plasma. Moreover, in order to supplement the genetic evidence, a comparative transcriptome analysis of liver was conducted to determine gene expression patterns related to elevation. Combining phenotype and genotype presents an intriguing and promising avenue for understanding animal adaptations to their environments. The present study contributes to revealing adaptive mechanisms at multiple levels in Chinese toads along an altitudinal gradient.

Results

Morphological parameters

High-altitude toads (at 2300 m and 3400 m) have smaller body size (both body mass and snout-vent length) than low-altitude individuals (at 1200 m and 50 m) (Additional file 1: Table S1). The dorsal skin structure of *B. gargarizans* at different altitudes was essentially the same, consisting of epidermis and dermis, and the order from body surface to deep layers was epidermis, loose and dense dermis (Fig. 2A). Pigments were mainly distributed in the stratum spongiosum of the dermis with only small amounts in the epidermis and stratum compactum of the dermis. Interestingly pigment cells were more regularly dispersed throughout the epidermis in high-altitude populations (at 2300 m and 3400 m) but were more aggregated in the low-altitude populations (at 50 m and 1200 m) (Fig. 2A). Changes in altitude did not affect the content of pigments (mean integrated optical density; MIOD) or the number of mucous glands (MGs) (Table 1). The epidermal thickness of *B. gargarizans* varied according to altitude ($P < 0.001$; Fig. 2B), being 17.5% ($P = 0.002$) at 2300 m and 57.5% ($P < 0.001$) at 3400 m higher than the value at 50 m, respectively. Moreover, the epidermal thickness at 3400 m was 40% ($P < 0.001$) and 34% ($P = 0.006$) greater than the values at 1200 m and 2300 m, respectively (Fig. 2B). The number of capillaries in the epidermis was not significantly different between three populations at altitudes of 1200 m, 2300 m and 3400 m, but each were markedly higher ($P < 0.01$) than the value for low-altitude toads (at 50 m) (Fig. 2C). The high-altitude population at 3400 m had 51.9% ($P = 0.012$) and 61.2% ($P = 0.005$) more GGs than the low-altitude populations (at 50 m and 1200 m), respectively (Fig. 2D). Changes in the altitudinal gradient significantly

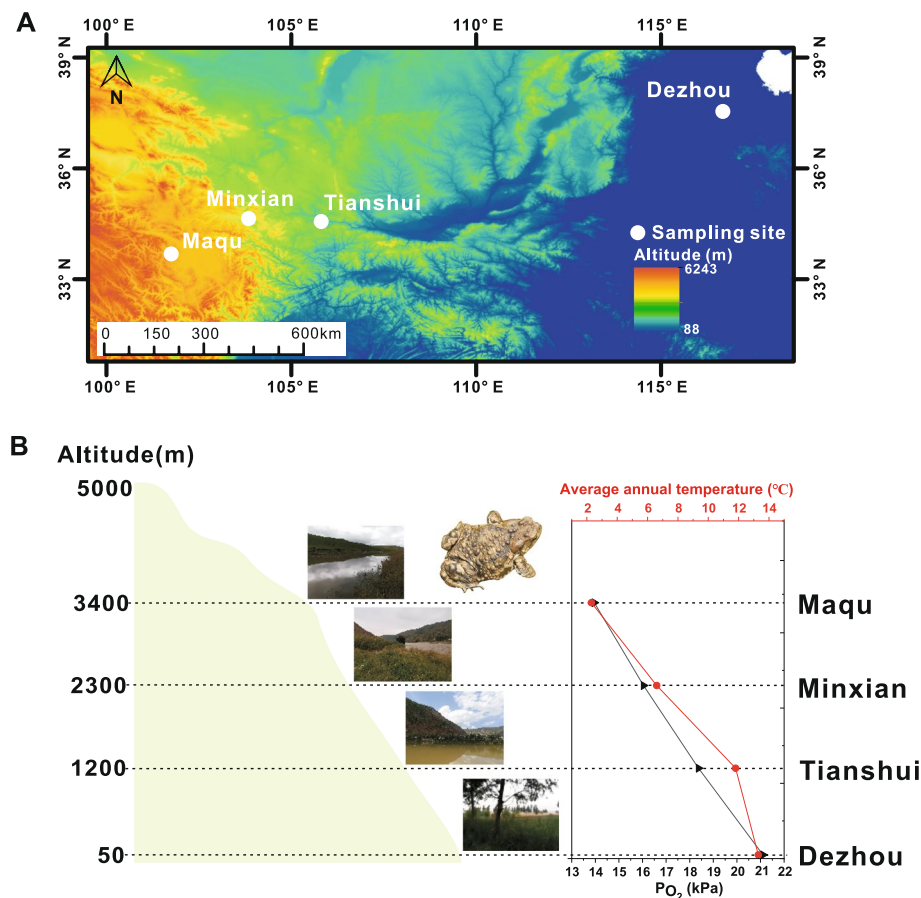


Fig. 1 **A** Schematic map of sampling sites and **(B)** landscape and ecological factors in wild habitats along the altitudinal gradient. Dezhou: 37.53°N, 116.78°E, 50 m a.s.l., Tianshui: 34.55°N, 105.91°E, 1200 m a.s.l., Minxian: 34.63°N, 103.97°E, 2300 m a.s.l., Maqu: 33.67°N, 101.87°E, 3400 m a.s.l.. Data for average annual temperature is from the National Meteorological Information Center of China (<http://data.cma.cn/>)

affected ($P < 0.001$) the length and width of GGs and MGs (Fig. 2E-2H). Neither the length and width of GGs nor the width of MGs differed significantly between high-altitude populations (at 2300 m and 3400 m), but these values were notably higher ($P < 0.05$) than those in low-altitude populations (at 50 m and 1200 m) (Fig. 2E, F, H). MGs in the three populations (at 1200 m, 2300 m and 3400 m) were significantly longer ($P < 0.05$) than those in low-altitude population (at 50 m), and the length of MGs at 3400 m was significantly higher ($P < 0.05$) than that at 1200 m (Fig. 2G).

Hematological parameters

Changes in altitude had a significant ($P < 0.001$) effect on all hematological indices tested (Table 2). As toad populations from 50 to 3400 m rose, the values for RBC counts, Hct, and [Hb] increased gradually and all were at their highest level in the 3400 m group ($P < 0.05$; Fig. 3A-C). There was no significant difference in the value of mean corpuscular hemoglobin concentration (MCHC)

among the lower altitudes of 50, 1200, and 2300 m, but the MCHC value at 3400 m was markedly higher ($P < 0.001$) than that at the other three altitudes (Fig. 3D). The value of mean corpuscular volume (MCV) decreased significantly ($P < 0.001$) with increasing altitude and was significantly lower at 3400 m than at the other three altitudes (Fig. 3E). The value of mean cell hemoglobin content (MCH) in three populations (at 1200 m, 2300 m, and 3400 m) were not significantly different but were all markedly lower ($P < 0.01$) than that of the low-altitude population (50 m) (Fig. 3F).

Antioxidants, metabolites, and metabolic network flux of CMP in the plasma

The activity of superoxide dismutase (SOD) and the content of vitamin C (Vc) and malondialdehyde (MDA) in the plasma were not affected by changing altitude (Table 3). However, the activity of catalase (CAT) was significantly higher ($P < 0.001$) at 3400 m than at the three other altitudes (Fig. 4A), with no significant

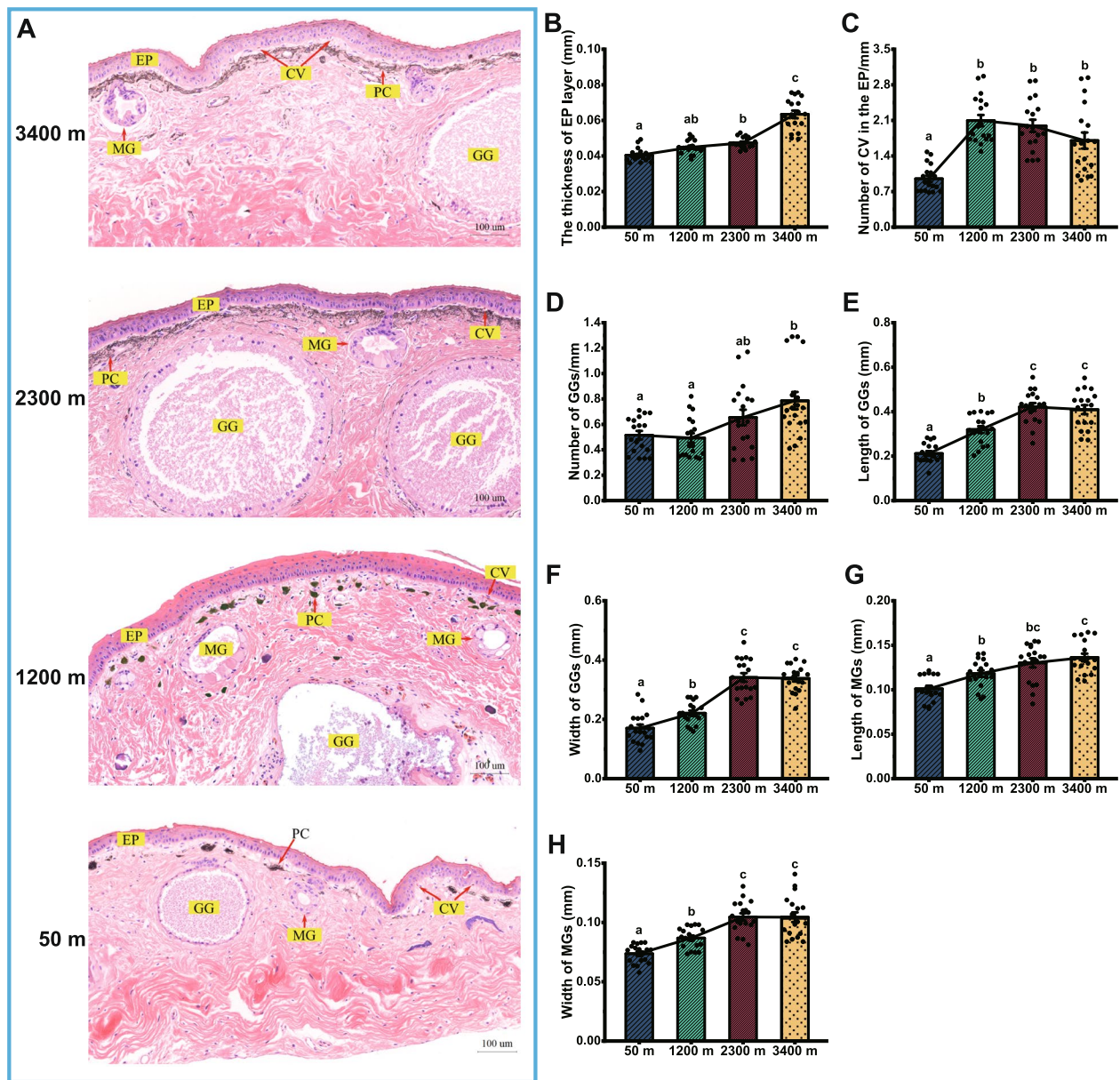


Fig. 2 A Dorsal skin structure of *B. gargarizans* from different altitudes and changes in histomorphological parameters; (B) thickness of the epidermis (EP) layer; (C) the number of CV in the epidermis; (D) total number of GGs; (E) length of GGs and (F) width of GGs, as well as (G) length of MGs and (H) width of MGs. PC, pigment cell. Data are expressed as means \pm SEM ($n = 18$). Different letters indicate statistically significant differences among the different altitudes at $P < 0.05$

Table 1 Results of non-parametric tests for the content of pigments (MIOD) and the number of mucous glands

	50 m	1200 m	2300 m	3400 m	P
Mean integrated optical density (MIOD)/mm	0.45 \pm 0.01	0.43 \pm 0.01	0.41 \pm 0.01	0.42 \pm 0.01	0.089
The number of mucous glands/mm	1.15 \pm 0.08	0.95 \pm 0.06	0.95 \pm 0.08	1.14 \pm 0.05	0.054

difference among the values for the three altitudes. The activity of glutathione peroxidase (GPX) and glutathione-S-transferase (GST) as well as total antioxidant capacity (T-AOC) were significantly affected ($P < 0.001$) by changing altitude (Fig. 4B-4D). GPX and GST activities as well as T-AOC showed no obvious differences between altitudes of 50 m and 1200 m, but these values increased significantly ($P < 0.001$) as altitude rose from 1200 to 3400 m.

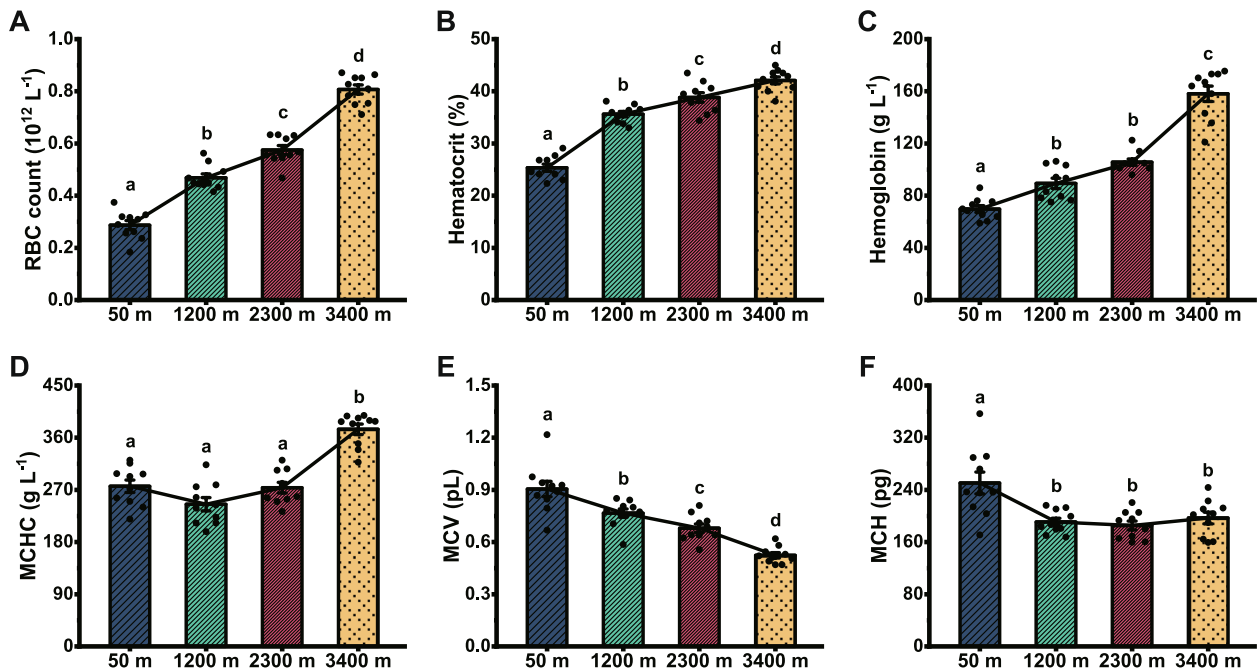


Fig. 3 Hematological parameters of *B. gargarizans* from different altitudes, including (A) RBCs counts, (B) Hct, (C) [Hb], (D) MCHC ([Hb]/Hct*100), (E) MCV (Hct/RBC count); and (F) MCH ([Hb]/RBC count). Data are expressed as the mean ± SEM (n = 10). Different letters indicate statistically significant differences among different altitudes at $P < 0.05$

Table 2 Summary of results from general linear models for hematological parameters

	RBC count		Hematocrit		Hemoglobin		MCHC		MCV		MCH	
	F	P	F	P	F	P	F	P	F	P	F	P
Intercept	107.319	< 0.001	309.593	< 0.001	94.156	< 0.001	120.513	< 0.001	134.332	< 0.001	93.372	< 0.001
Altitude	120.56	< 0.001	71.524	< 0.001	49.631	< 0.001	18.22	< 0.001	25.151	< 0.001	10.523	< 0.001
Body mass	4.656	0.038	0.546	0.465	< 0.001	0.996	0.208	0.651	4.23	0.047	4.545	0.04

Plasma metabolite levels were all significantly altered ($P < 0.001$) with altitude (Table 4). Glucose content at 50 m altitude was significantly higher than that at the other three altitudes, with 30.9% ($P < 0.001$), 21.7% ($P < 0.001$), and 14.5% ($P = 0.034$) lower levels seen at 1200 m, 2300 m and 3400 m, respectively (Fig. 4E). There was no significant difference in the content of either lactate or β -HB among the three populations (at 50 m, 1200 m and 2300 m), but both values at 3400 m were significantly higher ($P < 0.01$) than those at the three lower altitudes (Fig. 4F, 4G). The content of nicotinamide adenine dinucleotide (NADH) was the highest at 50 m altitude, being 30.8% ($P < 0.001$), 60.4% ($P < 0.001$), and 37.1% ($P < 0.001$) higher than the values at 1200 m, 2300 m, and 3400 m, respectively (Fig. 4H). There were no changes in the FFA content between 3400 and 1200 m. Compared to the value at 50 m, FFA content showed a 32% ($P < 0.001$), 20% ($P = 0.003$) and 40% ($P < 0.001$) reduction at 1200 m,

2300 m and 3400 m altitudes, respectively (Fig. 4I). After matrix calculation, CMP metabolic network flux maps were plotted for different populations of toads (Fig. 4J). As altitude rose from 50 to 3400 m, the metabolic flux of pentose phosphate pathway (PPP) gradually decreased from 37.04 to 2.23, whereas the metabolic flux of lactate increased from 124.23 to 192.38, and the metabolic flux of β -HB decreased from 3.25 to 1.67.

Differentially expressed genes (DEGs) identification and expression patterns related to altitude

RNA-seq analysis of 12 samples yielded a total of 80.21 GB of clean data, with more than 6.49 GB of clean data for each sample. The percentage of clean reads aligned to the reference genome sequence was greater than 76% (Additional file 1: Table S2). Principal component analysis showed a clear separation among toad populations from different altitudes (Fig. 5A). There were

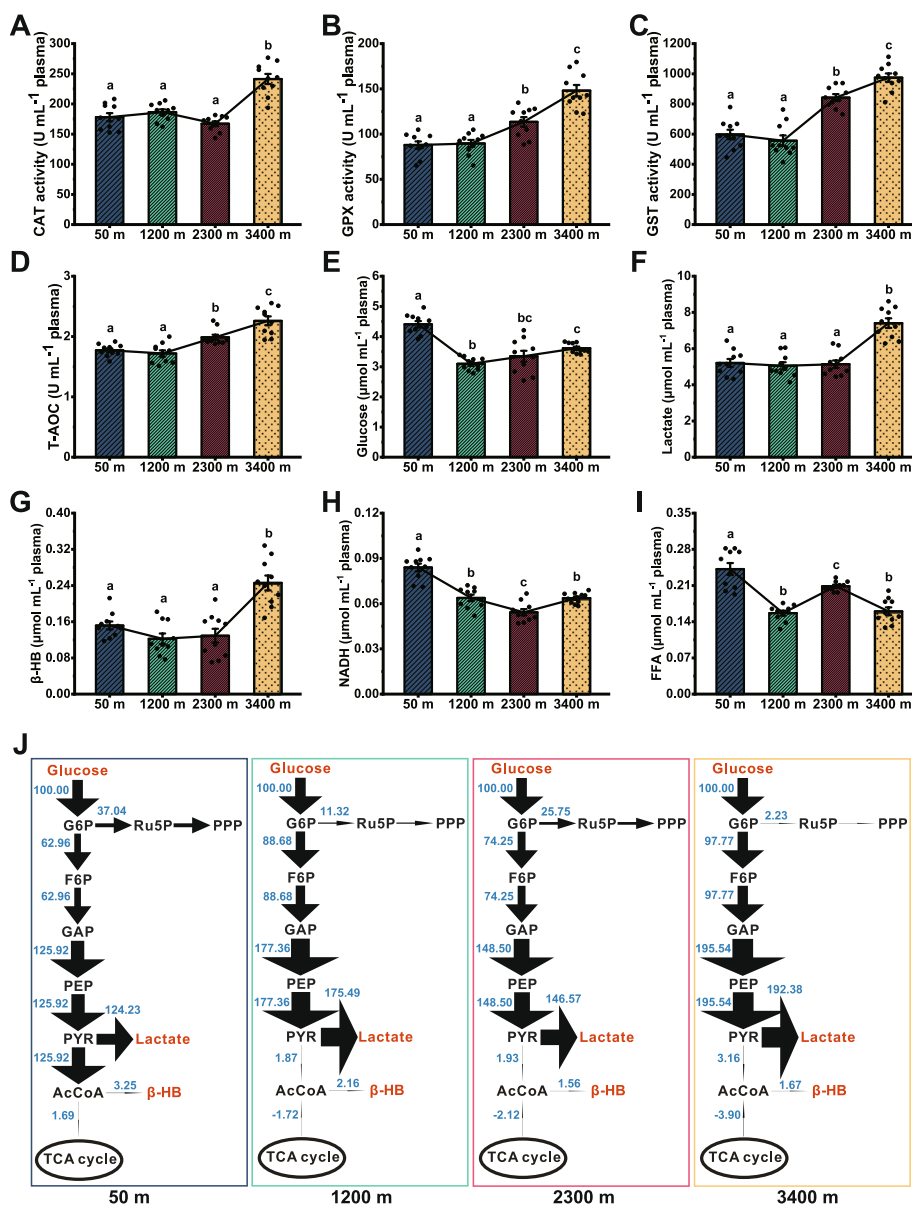


Fig. 4 Antioxidants, MDA, and metabolites in the plasma of *B. gargarizans* from different altitudes, including (A) CAT, (B) GPX, (C) GST, (D) T-AOC, (E) glucose, (F) lactate, (G) β-HB, (H) NADH, and (I) FFA. Data are expressed as means ± SEM (*n* = 10). Different letters indicate statistically significant differences among different altitudes at *P* < 0.05. **J** Metabolic network flux of the CMP in plasma of *B. gargarizans* from different altitudes. In the network, the thickness of lines represents the flux of metabolic pathways and arrows point in the direction of metabolic reactions

Table 3 Statistical analysis of general linear models for SOD, Vc, and MDA

	50 m	1200 m	2300 m	3400 m	<i>F</i>	<i>P</i>
SOD (U mL ⁻¹ plasma)	163.24 ± 4.22	157.23 ± 4.47	166.10 ± 4.07	177.00 ± 4.68	2.557	0.071
Vc (μg mL ⁻¹ plasma)	22.07 ± 1.02	20.01 ± 1.09	23.59 ± 0.99	24.77 ± 1.14	2.461	0.079
MDA (nmol mL ⁻¹ plasma)	5.14 ± 0.35	5.28 ± 0.37	4.21 ± 0.34	3.86 ± 0.39	2.101	0.118

Data are presented as adjusted mean values and standard errors

Table 4 Summary of results from general linear models for metabolites

	Glucose		Lactate		β-HB		NADH		FFA	
	F	P	F	P	F	P	F	P	F	P
Intercept	113.066	< 0.001	123.745	< 0.001	8.77	0.005	177.685	< 0.001	137.808	< 0.001
Altitude	24.972	< 0.001	15.549	< 0.001	17.42	< 0.001	34.281	< 0.001	33.409	< 0.001
Body mass	1.513	0.227	2.59	0.117	2.744	0.107	1.448	0.237	4.022	0.053

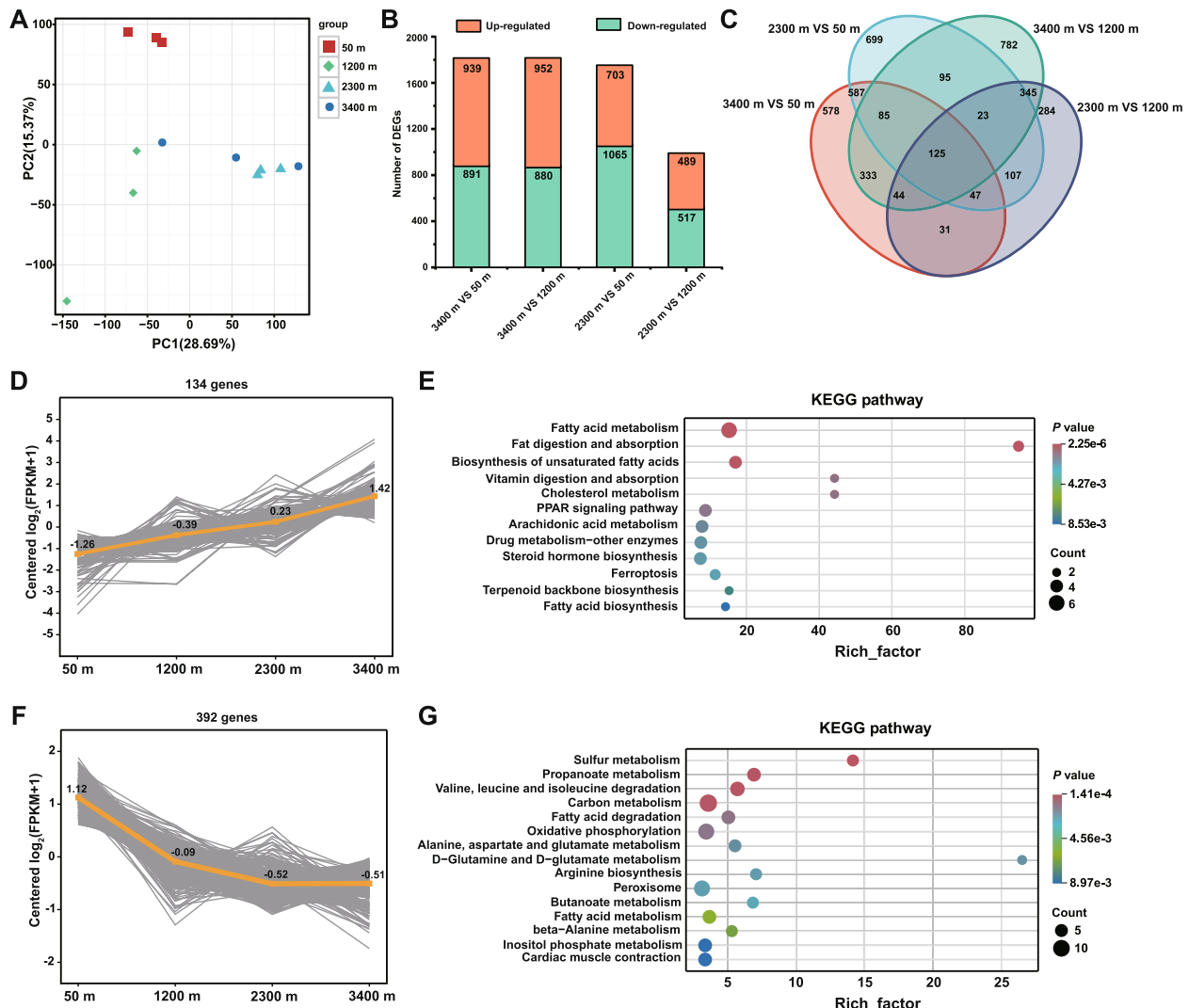


Fig. 5 **A** Principal component analysis of 12 individuals of *B. gargarizans* from four altitudes ($n=3$ for each group). **B** Number statistics and **(C)** Venn diagram of DEGs among four different comparisons. **D** K-means clustering identified a serially up-regulated pattern along the altitudinal gradient and **(E)** the enriched KEGG pathway for these genes. **F** K-means clustering identified a serially down-regulated pattern along the altitudinal gradient and **(G)** the enriched KEGG pathway for these genes

1830 DEGs in the comparison of 3400 m vs 50 m, 1832 DEGs in the comparison 3400 m vs 1200 m, 1768 DEGs in the comparison 2300 m vs 50 m, and 1006 DEGs in the comparison 2300 m vs 1200 m, respectively (Fig. 5B). In

total, we found that 125 DEGs were shared within the four comparisons (Fig. 5C; Additional file 1: Fig. S1). Gene Ontology (GO) enrichment analysis showed that the 125 shared DEGs were mainly enriched in unsaturated fatty

acid biosynthetic process, lipid transport, cholesterol transport, skin morphogenesis, and multiple metabolic processes in the biological process category (Additional file 1: Fig. S2), as well as 2-alkenal reductase [NAD(P)⁺] activity, phospholipase activity, stearoyl-CoA 9-desaturase activity, palmitoyl-CoA 9-desaturase activity, and fatty acid synthase activity in the molecular function category. Moreover, Kyoto Encyclopedia of Genes and Genomes (KEGG) enrichment analysis showed that 125 shared DEGs were significantly enriched in the pathway of fatty acid metabolism and biosynthesis of unsaturated fatty acids (Additional file 1: Fig. S2).

A cluster of 134 DEGs with a continuously up-regulated pattern along the altitudinal gradient was obtained (Fig. 5D) and these genes were significantly ($P < 0.01$) enriched in unsaturated fatty acid biosynthetic process, negative regulation of small molecule metabolic process, and lipid transport in the biological process category, as well as lipid transporter activity, iron ion binding, and aspartic-type endopeptidase activity in the molecular function category (Additional file 1: Fig. S3). KEGG pathway enrichment analysis showed that 134 continuously up-regulated genes were mainly enriched in the pathways involving fatty acid biosynthesis and metabolism, vitamin digestion and absorption, cholesterol metabolism, and PPAR signaling pathway (Fig. 5E). A cluster of 392 DEGs with a continuously down-regulated pattern along the altitudinal gradient was also discovered (Fig. 5F). GO enrichment analysis showed that these 392 DEGs were mainly enriched in carboxylic acid metabolic process, oxoacid metabolic process, organic acid metabolic process, fatty acid metabolic process, iron ion binding, oxidoreductase activity, heme binding, enoyl-CoA hydratase activity, ligase activity, and catalytic activity (Additional file 1: Fig. S4). KEGG pathway enrichment analysis showed that 392 continuously down-regulated genes were mainly enriched in carbon metabolism, sulfur metabolism, fatty acid metabolism, amino acid metabolism, oxidative phosphorylation, and cardiac muscle contraction (Fig. 5G).

Weighted gene co-expression network analysis (WGCNA) and key module identification

A total of 32 distinct co-expression modules were constructed (Additional file 1: Fig. S5). We found that 13 modules were significantly correlated with altitude ($P < 0.05$), among which the MEorangered4 module was the top positive correlation with altitude and most phenotypic traits. However, the MEyellowgreen module was the top negative correlation with altitude and several phenotypic traits (Additional file 1: Fig. S6). Moreover, MEyellowgreen and MEorangered4 modules were the top positively and negatively correlated with PO₂,

respectively. Subsequently, the MEorangered4 (Fig. 6A) and MEyellowgreen (Fig. 6B) modules were selected for GO and KEGG enrichment analyses, respectively. Genes in the MEorangered4 module were significantly enriched in GO terms including synapse organization, positive regulation of hypoxia-inducible factor-1alpha signaling pathway, translation, cell junction organization, synapse maturation, ureter development, response to nematode, positive regulation of protein sumoylation, structural constituent of ribosome, and glycosylphosphatidylinositol phospholipase D activity. In addition, KEGG pathway enrichment analysis showed that genes in the MEorangered4 module were mainly enriched in ribosome (Fig. 6C). GO enrichment analysis showed that genes in the MEyellowgreen module were significantly enriched in 60 terms in the biological process category, such as complement activation, regulation of complement activation, regulation of B cell mediated immunity, and regulation of immunoglobulin mediated immune response, as well as 25 terms in the molecular function category, and two KEGG pathways, including glycosphingolipid biosynthesis-lacto and neolacto series and glycosaminoglycan biosynthesis-keratan sulfate (Fig. 6D).

Discussion

Living at high altitude, *B. gargarizans* is able to withstand harsh environmental stresses, such as low oxygen partial pressure, low ambient temperature, and strong UVR, by virtue of a suite of histomorphological, physiological, biochemical, and molecular mechanisms.

Regarding morphological parameters, higher altitude toads have smaller body size (both body mass and snout-vent length), that follows the converse Bergmann's rule [31]. Lower temperatures, shortened activity seasons, and/or lower oxygen supply at higher altitudes result in delayed maturation and reproduction, as well as slower growth [32]. We attributed the decrease in body size with altitude to reduced growth rates at higher altitudes, since toads living at low altitudes grow faster than those living at moderate or high altitudes [30]. Regarding body masses, toads at higher altitudes have smaller body masses for two possible reasons: (1) toads prioritize energy allocation to reproductive activities rather than enhancing body masses during the breeding season; and (2) shorter foraging times due to a compressed activity period and lower daily temperatures, even with food shortages at higher altitude.

Amphibians rely heavily on their skin that provides great morpho-functional diversity in adapting to their living environment. The epidermis, that is in contact with the environment, not only produces a semi-permeable stratum corneum that plays a protective role but is also engaged in regulating ion exchange and acid-base

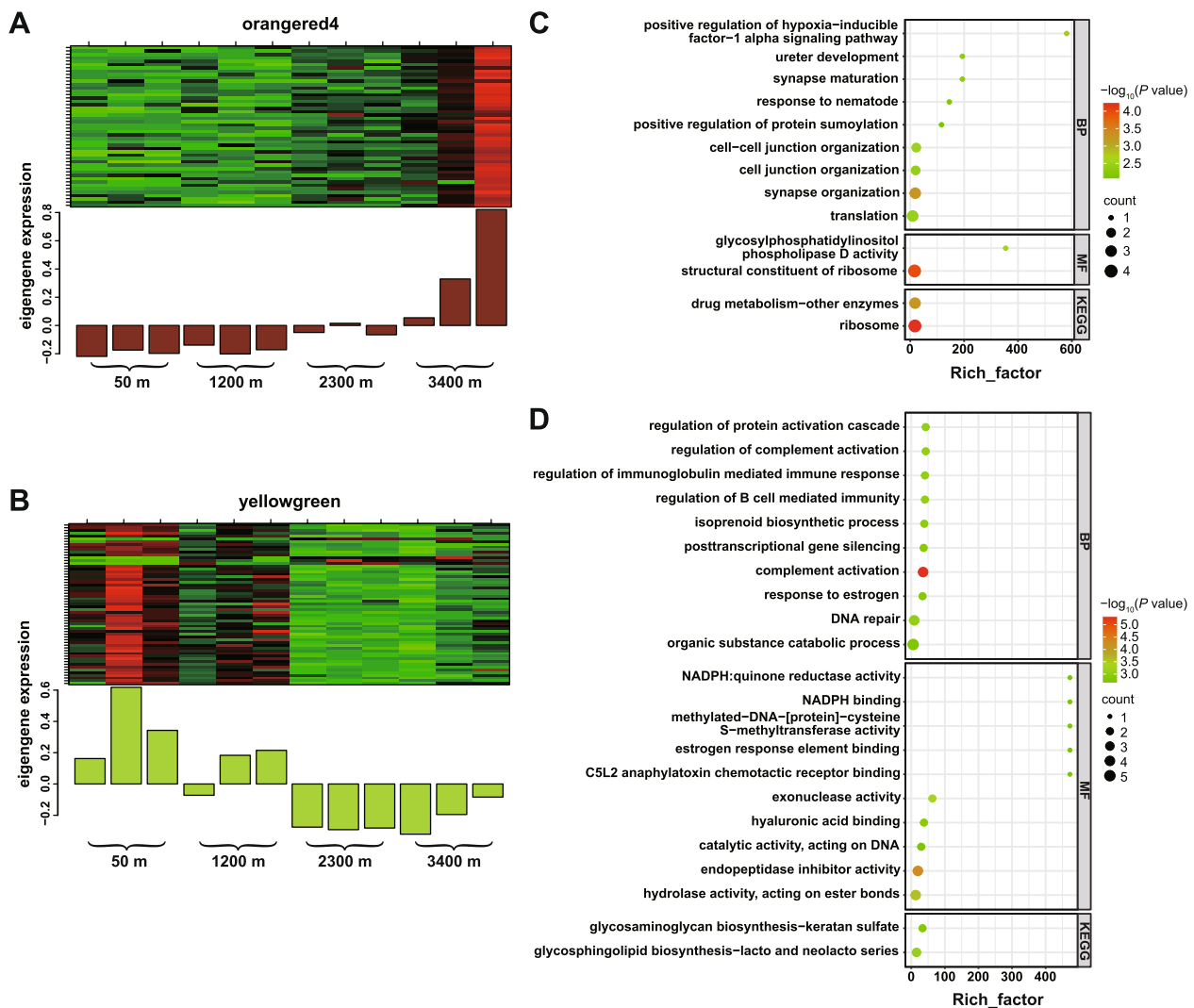


Fig. 6 The top significantly associated modules with the majority of phenotypic traits, including orangered4 and yellowgreen. Heatmap of gene co-expression within (A) orangered4 and (B) yellowgreen modules (upper panel) and the expression of corresponding eigengenes in each sample (lower panel). C The enriched GO terms biological process (BP) and molecular function (MF) and KEGG pathways for genes within the orangered4 module. D The top 10 enriched GO terms and KEGG pathways for genes within the yellowgreen module. The color shades represent different *P* values, and the size of the circle represents the gene numbers

balance of body fluids [33]. As expected, thickened epidermis in higher-altitude populations (at 2300 m and 3400 m) is beneficial in resisting intensified UVR, enduring external mechanical forces and preventing moisture loss. Similarly, a previous study showed that high-altitude individuals of the genus *Rana* had thicker skin than low-altitude individuals [34]. Skin capillaries can aid respiration by regulating cutaneous gas exchange (e.g., diffusion rates of oxygen and carbon dioxide) [6]. In the present study, richer capillaries can not only promote transcutaneous gas exchange, but also compensate for the negative effects of epidermal thickening in high-altitude toads, that is an important adjustment to deal with hypoxia

stress at high altitudes. Similarly, high-altitude *N. parkeri* frogs have more epidermal capillaries than other proximal frogs living at lower altitudes [10]. The thermal melanism hypothesis amply illustrates the importance of melanin in thermoregulation, cryptic coloration, protective coloration, defense against UVR, disease resistance, and sexual selection, to name a few [35]. Aggregating or dispersing melanin granules can effectively control skin color, with the former brightening the skin and the latter darkening it [36]. Intriguingly, higher altitude toads did not have significantly more melanin in their skin but deepened their skin tone via its dispersed distribution. Compared to aggregation, an even distribution of

melanin would provide a more effective defense against UVR for higher-altitude toads since darker skin can weaken ultraviolet penetration [37]. Moreover, in toads living in colder regions at higher altitudes, darker skin tones possess the advantage of faster heating according to the thermal melanism hypothesis [35]. This could allow for a more rapid elevation of body temperature for these ectothermic animals to help support foraging in cooler environments.

The GGs, also known as serous or venom glands, can produce a toxic or repellent secretion for defense functions [38]. In this study, more GGs in higher-altitude toads may help to secrete lipids to prevent the loss of body water, as already reported for the genus *Phyllomedusa* [39], since toads exposed to high altitude may suffer potentially greater dehydration than animals at lower elevations [40, 41]. Similarly, the number of GGs found in the plateau-dwelling frogs, *N. parkeri*, were greater than those in its lower-altitude counterparts [10]. However, in Andrew's toad, *B. andrewsi*, the MGs area in dorsal skin did not change significantly with altitude, but the GGs area was reduced with altitude, which may be due to lower predation pressure at high altitudes [42]. Thus, we tentatively propose that enlarging the size of MGs and GGs, as well as increasing the number of GGs, could help high-altitude toads produce and store more defensive substances, such as antimicrobial peptides [38], in order to protect against predators and invasions. Among the peptides secreted by the glands, many have already been described as potential anticancer therapeutics [43]. It is intriguing that larger and numerous glands with increasing altitude may lead to an increased output of anticancer peptides, that may be promising candidates for anticancer agents. Notably, shared DEGs were significantly enriched in the skin morphology process, in which the gene *LOC122928892* (encoding ERBB receptor feedback inhibitor 1 or EGF receptor inhibitor Mig-6) showed a significant decrease in mRNA expression with elevation. Mig6 is a negative regulator of EGF receptor-mediated skin morphogenesis and tumor formation, and its deletion leads to hyperproliferation and impaired differentiation of epidermal keratinocytes [44]. Moreover, UVR can accelerate skin aging, which is known as "photo-aging" [45]. Thus, it can be asserted that high-altitude toads showed more rapid skin aging relative to low-altitude individuals, where lower expression of Mig6 may be responsible. This gene could be an important target for the treatment of plateau-associated skin aging.

It is commonly observed that hematologic adjustments, including increasing the number of RBCs and raising [Hb], are used to improve oxygen-carrying capacity in animals living at high altitudes [13, 46]. Our results from the present study support this idea and coincide

with similar changing trends in a previous study [16]. Unexpectedly, the value of Hct increased gradually with altitude, which may be detrimental to circulation and oxygen transport since blood viscosity and peripheral vascular resistance would be increased. However, as compared with values reported in other amphibians, such as the bullfrog, *Rana catesbeiana*, that has a mean Hct of $40.40 \pm 1.2\%$ [47], the Hct was not much higher in high-altitude toads ($42.97 \pm 0.87\%$, at 3400 m). Moreover, animals can utilize cardiovascular compensatory mechanisms, such as elevated arterial blood pressure, to overcome increased blood viscosity caused by higher Hct [48]. Thus, greater Hct may not be a burden for blood oxygen transport and gas exchange in high-altitude toads.

As yet, the effects of exposure to high altitude on the antioxidant system among animals have not been harmonized. The activities of antioxidant enzymes (SOD, CAT, GPX, and GST) in high-altitude lizards, *Psammotromus algirus*, did not significantly differ from those in low-altitude individuals [49], supporting the idea that high altitudes do not affect the antioxidant system. Consistent with our expectations, high-altitude toad populations (at 2300 m and 3400 m) enhanced their antioxidant defenses by up-regulating the activity of antioxidant enzymes (CAT, GPX, GST). This adaptive strategy for life at high altitudes coincides with the widespread phenomenon of "preparation for oxidative stress" [50]. Similarly, high-altitude *N. parkeri* also have stronger antioxidant defenses than their low-altitude counterparts, exhibiting higher activity of SOD, CAT, GPX, and GST in the liver [15]. Surprisingly, altitudinal changes did not influence the activity of SOD and the content of Vc (a small molecule antioxidant). The liver is the most responsive tissue to oxidative damage and produces most of the antioxidant enzymes [51]. Therefore, plasma SOD activity did not vary with altitude, probably because there was no change in the expression of SOD in liver. Furthermore, Vc content did not change across the altitudinal gradient, possibly due to the similar food composition at all altitudes tested. Conforming to our expectations, there was also no significant change in MDA (a biomarker of oxidative damage) content along the altitudinal gradient, suggesting that the high-altitude environment did not induce oxidative damage owing to an enhanced antioxidant defense.

The present study also linked ascent to high altitude with a clear increase in lactate metabolic flux, suggesting a gradual shift from aerobic to anaerobic metabolism, that is consistent with a reduction in oxygen concentration with altitude. Moreover, a lower flux from acetyl-coenzyme A (AcCoA) into the TCA cycle also suggests a suppressed aerobic metabolism in high-altitude toads that is more conducive to reducing metabolic costs in a

stress-filled environment. In agreement with the transcriptomic results, continuously down-regulated genes were significantly enriched in carbon metabolism and oxidative phosphorylation. Moreover, a higher level of plasma lactate implies that the adaptation of *B. gargarizans* to high-altitude environments is associated with tolerance to the accumulation of anaerobic by-products. The decrease in metabolic flux from AcCoA into β -HB (an indicator of fatty acid metabolism) and the significant enrichment of both continuously down-regulated genes and 125 shared DEGs in the pathway of fatty acid metabolism suggest that fatty acid metabolism is down-regulated in high-altitude toads. Indeed, the overwhelming evidence for metabolic adaptation to high altitude has shown that fatty acid metabolism strongly declines [19, 52, 53]. These results also indicate a greater reliance on carbohydrates rather than fatty acids as fuel for survival in high-altitude environments. This is logical since mobilization of carbohydrates is more advantageous than fatty acids in low oxygen environments, where the former can be oxidized both aerobically and anaerobically whereas the latter can only be oxidized aerobically [54]. In addition, 125 shared DEGs were also significantly enriched in the pathway of biosynthesis of unsaturated fatty acids, potentially linked with lower temperatures at high altitude that contribute to a higher proportion of polyunsaturated fatty acids. This is in accord with the widely reported membrane adaptation hypothesis [55, 56]. Thus, future studies probing lipid composition and fatty acid ratios are needed.

It is well known that the transcriptional response to hypoxia is mediated by the hypoxia-inducible factor (HIF) signaling cascade at the cellular level [57, 58]. In this study, MEorangered4 was the top positively correlated module with altitude and many phenotypic traits and was significantly enriched in the positive regulation of the HIF-1 α signaling pathway. This result suggests that HIF-1 α signaling plays a crucial role in the adaptation of Chinese toads, *B. gargarizans*, to the hypoxic environment at high altitudes, and likely promotes the formation of new blood [59], the ability for oxygen utilization [60], and suppression of oxidative metabolism [53]. Also, it has been widely demonstrated that the HIF-1 α signaling pathway is up-regulated or activated in many native animals living at high-altitude, such as the lizard, *Laudakia sacra* [61], the frog, *N. parkeri* [62], and the fish, *Triplophysa scleroptera* [63]. Ribosomes, the site of protein synthesis, perform a variety of important physiological functions [64]. For instance, the translation of HIF-1 α is regulated in a ribosomal protein S6-dependent manner [65], and HIF-1 α mRNA contains an internal ribosome entry site that allows for a sustained and efficient translation under

hypoxic conditions. This, in turn, induces the transcription of many genes involved in the cellular response to hypoxia [66]. GO enrichment analysis showed that positively selected genes were associated with ribosomes in the lung of the plateau native yak (*Bos grunniens*) [67]. Accordingly, up-regulation of the ribosomal pathway was also crucial for Chinese toads to respond to stresses such as hypoxia and low temperature at high altitudes.

High-altitude environmental factors, such as hypobaric hypoxia, UVR, and low temperatures, can affect an animal's immune system [68]. Moreover, high-altitude adaptation correlated neatly with activation of the immune system, for example, up-regulated genes in high altitude-dwelling species were significantly enriched in the immunity pathway compared to their low-altitude counterparts [69]. However, the evidence of transcript levels showed that the immune system may be suppressed in high-altitude toads. Immunity is energetically expensive [70], so we provisionally deduced that immune suppression in high-altitude toads would contribute to decelerating the depletion of fuel/energy reserves in response to environmental stresses, particularly cold temperatures. Further studies are needed to verify the changes in immunological parameters along the altitudinal gradient.

Conclusions

In summary, we conducted a comparative study that integrated histomorphological, physiological, biochemical, and molecular evidence to reveal adaptations to different environments in a representative species, the Chinese toad (*B. gargarizans*). Divergent phenotypes and transcriptomic expression profiling were observed among four toad populations along an altitudinal gradient, and gene expression largely consolidated the phenotypic features. Consistent with the assumption, we found that harsh environmental conditions at high altitude stimulate self-protective mechanisms in *B. gargarizans*, including increased epidermal thickness and epidermal capillary number, increased numbers of GGs, enlarged MGs and GGs, increased erythrocytes and Hct, elevated [Hb], enhanced antioxidant defenses, suppressed aerobic metabolism, and activated hypoxia-inducible factor signaling cascade. Transcriptome analysis revealed that gene expression regulation of fatty acid metabolism and synthesis plays a vital role in the adaptation of *B. gargarizans* to high altitudes. Moreover, this is the first study to use metabolic flux analysis to reveal adaptations to different environments. Overall, this study provides novel insights into phenotypic adaptations and genetic mechanisms used by Chinese toads in response to heterogeneous environments caused by changing altitude.

Methods

Sample collection

Adult male Chinese toads (*B. gargarizans*) ($n=10$ from each of the four populations) were collected from locations at 50, 1200, 2300, and 3400 m a.s.l. in China in July (Fig. 1). According to the results of phylogenetic analyses [26], we inferred that these toads were from the same evolutionary clade. The morphological parameters of toads and geographic coordinates of the sampling sites are presented in Table S1. Toads were euthanized by pithing on site and blood samples were collected from the aortic arch using heparinized glass capillary tubes. Fresh blood was used immediately to determine hematological parameters, including [Hb] and Hct. A portion of the fresh blood (10 μ L) was also diluted with sterile saline solution (0.65%) and followed by cryo-transportation to the laboratory at Dezhou University where these samples were used for counting RBCs. Other aliquots of blood samples were centrifuged at 3,000 g for 10 min to collect plasma that was then flash-frozen in liquid nitrogen. Samples of dorsal skin (near the foramen magnum, 0.5×0.5 cm) of toads ($n=6$ per population) were excised and fixed in a 4% paraformaldehyde solution for use in analyzing skin histology. The liver was also removed and immediately frozen in liquid nitrogen. All plasma and liver samples were kept frozen in liquid nitrogen for transport to the laboratory and then stored at -80°C before analysis.

Skin histology and image digitization

Skin histology was examined following conventional hematoxylin–eosin staining procedures as reported previously [10]. After embedding, sectioning (5 μ m thickness), and staining, images of all histological sections were observed and photographed with a Nikon Eclipse E100 microscope at $\times 100$ magnification. Three non-overlapping views of each tissue section photograph were randomly selected for determining skin pigment content (MIOD), skin thickness (in millimeters), and the number of epidermal capillary vessels (CV) and glands using Image Pro-Plus[®] (IPP) software (version 6.0). Finally, each group contained 18 valid values for subsequent statistical analysis.

Hematological parameters

Hematological parameters were assayed as reported previously [15]. Briefly, blood was drawn from the carotid artery into a capillary tube, which was then centrifuged for 10 min at 3,000 g to determine the Hct. [Hb] was measured using a commercial kit (Nanjing Jiancheng Ltd. Co., China), and RBC counts were determined using a

Table 5 Mass balance equations of intermediate metabolites in the CMP network

Intermediate metabolites	Mass balance equations
G6P	$X1 = r_1 - r_2 - r_3$
F6P	$X2 = r_3 - r_4$
GAP	$X3 = r_4 - r_5$
PEP	$X4 = r_5 - r_6$
PYR	$X5 = r_6 - r_7 - r_8$
AcCoA	$X6 = r_8 - r_9 - r_{10}$

Abbreviations are G6P Glucose-6-phosphate, F6P Fructose-6-phosphate, GAP Glyceraldehyde-3-phosphate, PEP Phosphoenolpyruvate, PYR Pyruvate, AcCoA Acetyl-coenzyme A

hemocytometer (XB-K-25; Shanghai Qiuqing Biochemical Reagent and Instrument Co., Ltd., Shanghai, China) under a microscope.

Biochemical analysis

Oxidative damage and antioxidant defense indices, as well as metabolite levels, were assayed as described previously [71–73] with minor modifications. After frozen plasma was thawed ($n=10$ for each group), we assessed the oxidative damage marker (MDA) and antioxidant defense indices including SOD, CAT, GPX, GST, Vc, and T-AOC using commercial assay kits (Nanjing Jiancheng Ltd. Co., Nanjing, China). Moreover, the content of selected metabolites including glucose, lactate, β -HB, NADH, and FFA were determined using commercial assay kits from the same manufacturer. With the exception of FFA, that was measured using a UV–Vis spectrophotometer (UV-5100H, METASH, Shanghai, China), all other indicators were assessed using an automatic microplate reader (BioTek Instruments, Inc., Winooski, USA). All enzymatic assays were performed at $25 \pm 0.5^\circ\text{C}$. For each indicator, the order of all samples examined was randomized.

Constructing the network of CMP and analysis of metabolic flux

To quantitatively compare the metabolic state of Chinese toads along an altitudinal gradient, we built a metabolic network of CMP (Additional file 1: Fig. S7) with a total of 10 metabolic pathways (r_1 – r_{10}) containing glycolysis, PPP and TCA cycle according to the principles of metabolic network construction [74]. We presumed that six intermediate metabolites, including glucose-6-phosphate (G6P), fructose-6-phosphate (F6P), glyceraldehyde-3-phosphate (GAP), phosphoenolpyruvate (PEP), pyruvate (PYR), and AcCoA were all in pseudo-steady states according to the calculation principle of metabolic fluxes [74], so that they were not accumulated and were all

equal to zero in the corresponding mass balance equations (Table 5). Then, the absolute content of glucose, lactate, β -HB, and NADH was corrected for body mass and brought into the following matrix to calculate the values of metabolic flux of each pathway. Finally, the value of metabolic flux was normalized by r_1 that was defined as 100 and a directed weighted metabolic network was plotted [74].

$$\begin{bmatrix} r_2 \\ r_3 \\ r_4 \\ r_5 \\ r_6 \\ r_8 \\ r_9 \end{bmatrix} = \begin{bmatrix} 1 & -0.5 & -0.2 & -0.1 \\ 0 & 0.5 & 0.2 & 0.1 \\ 0 & 0.5 & 0.2 & 0.1 \\ 0 & 1 & 0.4 & 0.2 \\ 0 & 1 & 0.4 & 0.2 \\ 0 & 0 & 0.4 & 0.2 \\ 0 & 0 & -0.6 & 0.2 \end{bmatrix} \times \begin{bmatrix} r_1 \\ r_7 \\ r_{10} \\ p \end{bmatrix}$$

RNA extraction, transcriptome sequencing and analysis

Liver samples ($n=3$ for each sampling site) were used for RNA extraction as reported previously [75]. Briefly, after standard extraction, enrichment, library construction, and amplification, a paired-end 150-bp sequencing was conducted on an Illumina HiSeq 2,500 platform. Raw data was uploaded to the BMKCloud service (<http://www.biocloud.net/>) for data processing with FastQC and conducting a reference-based RNA-Seq analysis. Clean reads were mapped to the *B. gargarizans* reference genome with a BioProject accession number of PRJNA628553 (https://ftp.ncbi.nlm.nih.gov/genomes/all/GCF/014/858/855/GCF_01485885.1_ASM1485885v1/GCF_01485885.1_ASM1485885v1_genomic.fna.gz) [25]. The range of altitudes from 1500–2500 m is usually classified as high altitude [76], so we grouped the four altitudes into two high (2300 m and 3400 m) and two low (1200 m and 50 m) altitudes and created four sets of comparisons (3400 m vs 50 m, 3400 m vs 1200 m, 2300 m vs 50 m, 2300 m vs 1200 m). Fold change ≥ 2 and false discovery rate < 0.05 were used as criteria to screen DEGs. Then, a gene co-expression cluster analysis with k-means clustering was conducted to trace the changing pattern of DEGs along the altitudinal gradient. Clusters of DEGs with continuous changes (up or down) were targeted and then these DEGs were subjected to GO and KEGG enrichment analyses. Significant enrichment of GO terms and KEGG pathways was judged by a condition of $P < 0.01$. Moreover, we used a WGCNA to further identify gene modules that were highly associated with ecological factors (altitude, PO_2 , and mean annual temperature) and phenotypic features. Genes with low expression (mean fragments per kilobase of transcript per million mapped reads (FPKM) < 1) were filtered out. The mean values of each physiological and biochemical index were used

for WGCNA. The key parameters of WGCNA were set as follows: softPower=13, TOMType=unsigned, min-ModuleSize=30, and mergeCutHeight=0.25. In addition, Pearson's correlation coefficient was calculated to determine the correlation between modules and ecological factors, and phenotypic features. Then, significantly correlated modules potentially explaining ecological and phenotypic variation were selected for GO and KEGG enrichment analyses with a criterion of $P < 0.01$.

Statistical analyses

All data were analyzed using SPSS 22.0 software (SPSS, Inc., Chicago, Illinois, USA). Normality and homogeneity of variances were tested using Shapiro–Wilk' test and Levene's test, respectively. Body mass and snout-vent length were tested using a one-way analysis of variance (ANOVA) followed by Dunnett's T3 post-hoc test for multiple comparisons. Among the histomorphological parameters, except for the length and width of the GGs, which were tested using ANOVA followed by Bonferroni's multiple comparison post-hoc test to compare differences between the four altitude groups, all other indices were tested using the non-parametric Kruskal–Wallis test by ranks. Hematological parameters and other physiological indices were tested using a general linear model (GLM) followed by Bonferroni-corrected pairwise comparisons with altitude as a fixed factor and body mass as a covariate. A significance level of $P < 0.05$ was accepted in all cases.

Abbreviations

UVR	Ultraviolet radiation
[Hb]	Hemoglobin concentration
Hct	Hematocrit
RBC	Red blood cell
TCA	Tricarboxylic acid
FFA	Free fatty acids
β -HB	β -Hydroxybutyric acid
CMP	Central metabolic pathway
MIOD	Mean integrated optical density
MGs	Mucous glands
GGs	Granular glands
MCHC	Mean corpuscular hemoglobin concentration
MCV	Mean corpuscular volume
MCH	Mean cell hemoglobin content
SOD	Superoxide dismutase
Vc	Vitamin C
MDA	Malondialdehyde
CAT	Catalase
GPX	Glutathione peroxidase
GST	Glutathione-S-transferase
T-AOC	Total antioxidant capacity
NADH	Nicotinamide adenine dinucleotide
PPP	Pentose phosphate pathway
DEGs	Differentially expressed genes
AcCoA	Acetyl-coenzyme A
HIF	Hypoxia-inducible factor
CV	Capillary vessels
G6P	Glucose-6-phosphate
F6P	Fructose-6-phosphate
GAP	Glyceraldehyde-3-phosphate

PEP	Phosphoenolpyruvate
PYR	Pyruvate
WGCNA	Weighted gene co-expression network analysis
GO	Gene Ontology
KEGG	Kyoto Encyclopedia of Genes and Genomes
FPKM	Fragments per kilobase of transcript per million mapped reads

Supplementary Information

The online version contains supplementary material available at <https://doi.org/10.1186/s12915-024-02033-6>.

Additional File 1: Table S1-S2 and Figures S1-S7. Table S1. Morphological parameters of toads and geographic coordinates of the sampling sites in this study. Table S2. Summary of RNA-seq quality data of 12 samples in *B. gargarizans* from four altitudes. Fig. S1. The heat map diagram showing changes in abundance of shared differentially expressed genes at four altitudes ($n = 3$ for each group). The FPKM values were log-normalized. Red color indicates highly expressed genes, and blue indicates low expressed genes. Fig. S2. The top 10 enriched GO terms and KEGG pathways for 125 shared DEGs in the liver. The color shades represent different P values, and the size of the circle represents the number of DEGs. Fig. S3. The top 10 enriched GO terms for a cluster of 134 DEGs with a continuous up-regulated pattern along the altitudinal gradient. The color shades represent different P values, and the size of the circle represents the number of DEGs. Fig. S4. The top 10 enriched GO terms for a cluster of 392 DEGs with a continuous down-regulated pattern along the altitudinal gradient. The color shades represent different P values, and the size of the circle represents the number of DEGs. Fig. S5. Cluster dendrogram of genes obtained through topological overlap matrix (TOM). Below the dendrogram, the first row represents the assigned original modules while the second row displays the merged modules. Fig. S6. The correlation between modules and ecological factors, and phenotypic features using WGCNA. The rows represent the 32 gene modules, and the columns show 3 ecological factors and 27 phenotypic features. AAT: average annual temperature; TEP: the thickness of epidermis layer; GGSL: the length of granular glands; GGW: the width of granular glands; MGSL: the length of mucous glands; MGW: the width of mucous glands. Fig. S7. A metabolic network of CMP with 10 pathways (r1-r10). These pathways include glycolysis, PPP and TCA cycle, in which metabolites include Ru5P, G6P, F6P, GAP, PEP, PYR, and AcCoA.

Acknowledgements

The authors wish to acknowledge Jinzhou Wang for the help with the fieldwork.

Authors' contributions

Y.G.N. conceived and designed the project. Y.G.N., X.J.Z., H.Y.Z., T.S.X., and X.Y.L. performed the experiments. Y.G.N., X.J.Z., L.W., and H.S.W. analyzed the data. Y.G.N., S.K.M., and L.D. collected the samples. Y.G.N. and X.J.Z. prepared the first draft of the manuscript. K.B.S., and Q.C. reviewed and edited the manuscript. All authors read and approved the final manuscript.

Funding

This work was supported by the National Natural Science Foundation of China (no. 32001110).

Availability of data and materials

All data generated or analyzed during this study are included in this published article, its supplementary information files and publicly available repositories. Raw sequence data was deposited in the Genome Sequence Archive (GSA) database (<https://ngdc.cnpc.ac.cn/gsa/>); accession number of PRJCA023477. The datasets generated and/or analyzed during this study are available in the figshare repository (<https://doi.org/10.6084/m9.figshare.25953943.v1>). Moreover, the reference genome of *B. gargarizans* was downloaded from NCBI with BioProject accession number PRJNA628553 for transcriptome analysis.

Declarations

Ethics approval and consent to participate

All procedures were approved by the Ethics Committee of Animal Experiments at Dezhou University (Approval No. DZXY2021004) and in accordance with guidelines from the China Council on Animal Care.

Consent for publication

Not applicable.

Competing interests

The authors declare that they have no competing interests.

Author details

¹School of Life Sciences, Dezhou University, Dezhou, Shandong 253023, China. ²School of Life Sciences, Lanzhou University, Lanzhou 730000, China. ³School of Life Science and Engineering, Southwest University of Science and Technology, Mianyang 621010, China. ⁴Department of Biology, Carleton University, Ottawa, ON K1S 5B6, Canada.

Received: 26 February 2024 Accepted: 3 October 2024

Published online: 10 October 2024

References

- Körner C. The use of 'altitude' in ecological research. *Trends Ecol Evol.* 2007;22:569–74.
- Ashton KG, Feldman CR. Bergmann's rule in nonavian reptiles: turtles follow it, lizards and snakes reverse it. *Evolution.* 2003;57:1151–63.
- Burggren WW, West NH. Changing respiratory importance of gills, lungs and skin during metamorphosis in the bullfrog *Rana catesbeiana*. *Respir Physiol.* 1982;47:151–64.
- Varga JF, Bui-Marinos MP, Katzenback BA. Frog skin innate immune defences: sensing and surviving pathogens. *Front Immunol.* 2019;9:433806.
- Arredondo J, González-Morales JC, Rodríguez-Antolín J, Bastiaans E, Monroy-Vilchis O, Manjarrez J, et al. Histological characteristics of gills and dorsal skin in *Ambystoma leorae* and *Ambystoma rivulare*: Morphological changes for living at high altitude. *Int J Morphol.* 2017;35:1590–6.
- Goniakowska-Witalińska L, Kubiczek U. The structure of the skin of the tree frog (*Hyla arborea arborea* L.). *Ann Anat.* 1998;180:237–46.
- Wanninger M, Schwaha T, Heiss E. Form and function of the skin glands in the Himalayan newt *Tylotriton verrucosus*. *Zoological Lett.* 2018;4:1–10.
- Guangming G, Tao Z, Chao L, Moyan Z. Different morphologic formation patterns of dark patches in the black-spotted frog (*Pelophylax nigromaculata*) and the Asiatic toad (*Bufo gargarizans*). *Anat Sci Int.* 2017;92:130–41.
- Reguera S, Zamora-Camacho FJ, Moreno-Rueda G. The lizard *Psammotromus algirus* (Squamata: Lacertidae) is darker at high altitudes. *Biol J Linn Soc Lond.* 2014;112:132–41.
- Yang C, Fu T, Lan X, Zhang Y, Nneji LM, Murphy RW, et al. Comparative skin histology of frogs reveals high-elevation adaptation of the Tibetan *Nanorana parkeri*. *Asian Herpetol Res.* 2019;10:79–85.
- González-Morales JC, Beamonte-Barrientos R, Bastiaans E, Guevara-Flore P, Quintana E, Fajardo V. A mountain or a plateau? Hematological traits vary nonlinearly with altitude in a highland lizard. *Physiol Biochem Zool.* 2017;90:638–45.
- Hutchison VH, Haines HB, Engbretson G. Aquatic life at high altitude: respiratory adaptations in the Lake Titicaca frog, *Telmatobius culeus*. *Respir Physiol.* 1976;27:115–29.
- Lu S, Xin Y, Tang X, Yue F, Wang H, Bai Y, et al. Differences in hematological traits between high- and low-altitude lizards (Genus *Phrynocephalus*). *PLoS One.* 2015;10:e0125751.
- Ma M, Pu P, Niu Z, Zhang T, Wu J, Tang X, et al. A novel mechanism for high-altitude adaptation in hemoglobin of black-spotted frog (*Pelophylax nigromaculatus*). *Front Ecol Evol.* 2023;11:1103406.
- Niu Y, Zhang X, Xu T, Li X, Zhang H, Wu A, et al. Physiological and biochemical adaptations to high altitude in Tibetan frogs, *Nanorana parkeri*. *Front Physiol.* 2022;13:942037.

16. Pu P, Zhao Y, Niu Z, Cao W, Zhang T, He J, et al. Comparison of hematological traits and oxygenation properties of hemoglobins from highland and lowland Asiatic toad (*Bufo gargarizans*). *J Comp Physiol B*. 2021;191:1019–29.
17. Bickler PE, Buck LT. Hypoxia tolerance in reptiles, amphibians, and fishes: life with variable oxygen availability. *Annu Rev Physiol*. 2007;69:145–70.
18. Tang X, Xin Y, Wang H, Li W, Zhang Y, Liang S, et al. Metabolic characteristics and response to high altitude in *Phrynocephalus erythrurus* (Lacertilia: Agamidae), a lizard dwell at altitudes higher than any other living lizards in the world. *PLoS One*. 2013;8:e71976.
19. Zhang X, Men S, Jia L, Tang X, Storey KB, Niu Y, et al. Comparative metabolomics analysis reveals high-altitude adaptations in a toad-headed viviparous lizard, *Phrynocephalus vlangalii*. *Front Zool*. 2023;20:35.
20. Birben E, Sahiner UM, Sackesen C, Erzurum S, Kalayci O. Oxidative stress and antioxidant defense. *World Allergy Organ J*. 2012;5:9–19.
21. Horgan RP, Kenny LC. Omic technologies: genomics, transcriptomics, proteomics and metabolomics. *Obstet Gynaecol*. 2011;13:189–95.
22. Yang Y, Wang L, Han J, Tang X, Ma M, Wang K, et al. Comparative transcriptomic analysis revealed adaptation mechanism of *Phrynocephalus erythrurus*, the highest altitude lizard living in the Qinghai-Tibet Plateau. *BMC Evol Biol*. 2015;15:1–14.
23. Yang W, Qi Y, Fu J. Genetic signals of high-altitude adaptation in amphibians: a comparative transcriptome analysis. *BMC Genet*. 2016;17:1–10.
24. Yang W, Qi Y, Lu B, Qiao L, Wu Y, Fu J. Gene expression variations in high-altitude adaptation: a case study of the Asiatic toad (*Bufo gargarizans*). *BMC Genet*. 2017;18:1–8.
25. Lu B, Jiang J, Wu H, Chen X, Song X, Liao W, et al. A large genome with chromosome-scale assembly sheds light on the evolutionary success of a true toad (*Bufo gargarizans*). *NCBI BioProject*. <https://www.ncbi.nlm.nih.gov/bioproject/PRJNA628553/>. 2021.
26. Othman SN, Litvinchuk SN, Maslova I, Dahn H, Messenger KR, Andersen D, et al. From Gondwana to the Yellow Sea, evolutionary diversifications of true toads *Bufo* sp. in the Eastern Palearctic and a revisit of species boundaries for Asian lineages. *Elife*. 2022;11:e70494.
27. Fu J, Weadick CJ, Zeng X, Wang Y, Liu Z, Zheng Y, et al. Phylogeographic analysis of the *Bufo gargarizans* species complex: a revisit. *Mol Phylogeny Evol*. 2005;37:202–13.
28. Zhang L, Chen J, Zhao R, Zhong J, Lin L, Li H, et al. Genomic insights into local adaptation in the Asiatic toad *Bufo gargarizans*, and its genomic offset to climate warming. *Evol Appl*. 2023;16:1071–83.
29. Chen Y, Tan S, Fu J. Modified metabolism and response to UV radiation: Gene expression variations along an elevational gradient in the Asiatic toad (*Bufo gargarizans*). *J Mol Evol*. 2022;90:389–99.
30. Tan S, Li P, Yao Z, Liu G, Yue B, Fu J, et al. Metabolic cold adaptation in the Asiatic toad: intraspecific comparison along an altitudinal gradient. *J Comp Physiol B*. 2021;191:765–76.
31. Mousseau TA. Ectotherms follow the converse to Bergmann's rule. *Evolution*. 1997;51:630–2.
32. Morrison C, Hero JM. Geographic variation in life-history characteristics of amphibians: a review. *J Anim Ecol*. 2003;72:270–9.
33. Madison KC. Barrier function of the skin: "la raison d'être" of the epidermis. *J Invest Dermatol*. 2003;121:231–41.
34. Mi Z, Liao W. Comparison of skin histostructures in three species of genus *Rana*. *Chin J Zool*. 2016;51:844–52.
35. Trullas SC, van Wyk JH, Spotila JR. Thermal melanism in ectotherms. *J Therm Biol*. 2007;32:235–45.
36. de Velasco JB, Tattersall GJ. The influence of hypoxia on the thermal sensitivity of skin colouration in the bearded dragon, *Pogona vitticeps*. *J Comp Physiol B*. 2008;178:867–75.
37. D'Orazio J, Jarrett S, Amaro-Ortiz A, Scott T. UV radiation and the skin. *Int J Mol Sci*. 2013;14:12222–48.
38. Toledo Rd, Jared C. Cutaneous granular glands and amphibian venoms. *Comp Biochem Physiol A Physiol*. 1995;111:1–29.
39. Blaylock LA, Ruibal R, Platt-Aloia K. Skin structure and wiping behavior of phyllomedusine frogs. *Copeia*. 1976:283–95.
40. Biswas H, Boral M. Changes of body fluid and hematology in toad and their rehabilitation following intermittent exposure to simulated high altitude. *Int J Biometeorol*. 1986;30:189–97.
41. Yao Z, Qi Y, Yue B, Fu J. Brain size variation along altitudinal gradients in the Asiatic Toad (*Bufo gargarizans*). *Ecol Evol*. 2021;11:3015–27.
42. Wang C, Jin L, Mi Z, Liao W. Geographic variation in skin structure in male Andrew's toad (*Bufo andrewsi*). *Anim Biol*. 2020;70:159–74.
43. Lu C, Nan K, Lei Y. Agents from amphibians with anticancer properties. *Anticancer Drugs*. 2008;19:931–9.
44. Ferby I, Reschke M, Kudlacek O, Knyazev P, Panté G, Amann K, et al. Mig6 is a negative regulator of EGF receptor-mediated skin morphogenesis and tumor formation. *Nat Med*. 2006;12:568–73.
45. Fisher GJ, Kang S, Varani J, Bata-Csorgo Z, Wan Y, Datta S, et al. Mechanisms of photoaging and chronological skin aging. *Arch Dermatol*. 2002;138:1462–70.
46. Ruiz G, Rosenmann M, Veloso A. Respiratory and hematological adaptations to high altitude in Telmatobius frogs from the Chilean Andes. *Comp Biochem Physiol A Physiol*. 1983;76:109–13.
47. Carmena-Suero A, Siret JR, Caixejas J, Arpones-Carmena D. Blood volume in male *Hyla septentrionalis* (tree frog) and *Rana catesbeiana* (bullfrog). *Comp Biochem Physiol A Physiol*. 1980;67:187–9.
48. Gallagher P, Farrell A. Hematocrit and blood oxygen-carrying capacity. In: *Fish physiology*. San Diego: Academic Press; 1998. p. 185–227.
49. Reguera S, Zamora-Camacho FJ, Trenzado CE, Sanz A, Moreno-Rueda G. Oxidative stress decreases with elevation in the lizard *Psammadromus algericus*. *Comp Biochem Physiol A Mol Integr Physiol*. 2014;172:52–6.
50. Moreira DC, Oliveira MF, Liz-Guimarães L, Diniz-Rojas N, Campos EG, Hermes-Lima M. Current trends and research challenges regarding "Preparation for Oxidative Stress." *Front Physiol*. 2017;8:702.
51. Casas-Grajales S, Muriel P. The liver, oxidative stress, and antioxidants. In: *Liver pathophysiology*. Waltham: Academic Press; 2017. p. 583–604.
52. Ge RL, Simonson TS, Gordeuk V, Prchal JT, McClain DA. Metabolic aspects of high-altitude adaptation in Tibetans. *Exp Physiol*. 2015;100:1247–55.
53. Murray AJ, Montgomery HE, Feelisch M, Grocott MP, Martin DS. Metabolic adjustment to high-altitude hypoxia: from genetic signals to physiological implications. *Biochem Soc Trans*. 2018;46:599–607.
54. Ge RL, Simonson TS, Cooksey RC, Tanna U, Qin G, Huff CD, et al. Metabolic insight into mechanisms of high-altitude adaptation in Tibetans. *Mol Genet Metab*. 2012;106:244–7.
55. Hazel JR. Thermal adaptation in biological membranes: is homeoviscous adaptation the explanation? *Annu Rev Physiol*. 1995;57:19–42.
56. Cossins A, Prosser C. Evolutionary adaptation of membranes to temperature. *Proc Natl Acad Sci U S A*. 1978;75:2040–3.
57. Semenza GL. Regulation of oxygen homeostasis by hypoxia-inducible factor 1. *Physiology*. 2009;24:97–106.
58. Semenza GL. HIF-1 and mechanisms of hypoxia sensing. *Curr Opin Cell Biol*. 2001;13:167–71.
59. Koh MY, Spivak-Kroizman TR, Powis G. HIF-1 regulation: not so easy come, easy go. *Trends Biochem Sci*. 2008;33:526–34.
60. Zhao P, He Z, Xi Q, Sun H, Luo Y, Wang J, et al. Variations in HIF-1 α contributed to high altitude hypoxia adaptation via affected oxygen metabolism in Tibetan sheep. *Animals*. 2021;12:58.
61. Yan C, Zhang Z, Lv Y, Wang Z, Jiang K, Li J. Genome of *Laudakia sacra* provides new insights into high-altitude adaptation of ectotherms. *Int J Mol Sci*. 2022;23:10081.
62. Zhang Q, Han X, Ye Y, Kraus RH, Fan L, Yang L, Tao Y. Expression of HIF-1 α and its target genes in the *Nanorana parkeri* heart: implications for high altitude adaptation. *Asian Herpetol Res*. 2016;7:12–20.
63. Chen J, Shen Y, Wang J, Ouyang G, Kang J, Lv W, et al. Analysis of multiplicity of hypoxia-inducible factors in the evolution of triplophysa fish (*Osteichthyes: Nemacheilinae*) reveals hypoxic environments adaptation to Tibetan plateau. *Front Genet*. 2020;11:433.
64. Brar GA, Weissman JS. Ribosome profiling reveals the what, when, where and how of protein synthesis. *Nat Rev Mol Cell Biol*. 2015;16:651–64.
65. Zhang D, Liu J, Mi X, Liang Y, Li J, Huang C. The N-terminal region of p27 inhibits HIF-1 α protein translation in ribosomal protein S6-dependent manner by regulating PHLPP-Ras-ERK-p90RSK axis. *Cell Death Dis*. 2014;5:e1535.
66. Lang KJ, Kappel A, Goodall GJ. Hypoxia-inducible factor-1 α mRNA contains an internal ribosome entry site that allows efficient translation during normoxia and hypoxia. *Mol Biol Cell*. 2002;13:1792–801.
67. Lan D, Xiong X, Ji W, Li J, Mipam TD, Ai Y, et al. Transcriptome profile and unique genetic evolution of positively selected genes in yak lungs. *Genetica*. 2018;146:151–60.
68. Mishra K, Ganju L. Influence of high altitude exposure on the immune system: a review. *Immunol Invest*. 2010;39:219–34.

69. Xin J, Chai Z, Zhang C, Zhang Q, Zhu Y, Cao H, et al. Transcriptome profiles revealed the mechanisms underlying the adaptation of yak to high-altitude environments. *Sci Rep.* 2019;9:7558.
70. Ganeshan K, Nikkanen J, Man K, Leong YA, Sogawa Y, Maschek JA, et al. Energetic trade-offs and hypometabolic states promote disease tolerance. *Cell.* 2019;177:399–413.
71. Niu Y, Zhang X, Zhang H, Xu T, Men S, Storey KB, et al. Antioxidant and non-specific immune defenses in partially freeze-tolerant Xizang plateau frogs, *Nanorana parkeri*. *J Therm Biol.* 2021;102:103132.
72. Zhang H, Zhang X, Xu T, Li X, Storey KB, Chen Q, et al. Effects of acute heat exposure on oxidative stress and antioxidant defenses in overwintering frogs, *Nanorana parkeri*. *J Therm Biol.* 2022;110:103355.
73. Niu Y, Chen Q, Storey KB, Teng L, Li X, Xu T, et al. Physiological ecology of winter hibernation by the high-altitude frog *Nanorana parkeri*. *Physiol Biochem Zool.* 2022;95:201–11.
74. Stephanopoulos G, Aristidou AA, Nielsen J. *Metabolic engineering: principles and methodologies.* San Diego: Academic Press; 1998.
75. Niu Y, Zhang X, Men S, Storey KB, Chen Q. Integrated analysis of transcriptome and metabolome data reveals insights for molecular mechanisms in overwintering Tibetan frogs, *Nanorana parkeri*. *Front Physiol.* 2023;13:1104476.
76. Wilson MH, Newman S, Imray CH. The cerebral effects of ascent to high altitudes. *Lancet Neurol.* 2009;8:175–91.

Publisher's Note

Springer Nature remains neutral with regard to jurisdictional claims in published maps and institutional affiliations.